SYNTHESIS OF THERMAL INTERFACE MATERIALS MADE OF METAL DECORATED CARBON NANOTUBES AND POLYMERS

A Thesis

by

MARION ODUL OKOTH

Submitted to the Office of Graduate Studies of
Texas A&M University
in partial fulfillment of the requirements for the degree of

MASTER OF SCIENCE

August 2010

Major Subject: Mechanical Engineering

SYNTHESIS OF THERMAL INTERFACE MATERIALS MADE OF METAL DECORATED CARBON NANOTUBES AND POLYMERS

A Thesis

by

MARION ODUL OKOTH

Submitted to the Office of Graduate Studies of
Texas A&M University
in partial fulfillment of the requirements for the degree of

MASTER OF SCIENCE

Approved by:

Chair of Committee,	Choongho Yu
Committee Members,	Xinghang Zhang
	Wenhao Wu
Head of Department,	Dennis O'Neal

August 2010

Major Subject: Mechanical Engineering

ABSTRACT

Synthesis of Thermal Interface Materials Made of Metal Decorated Carbon Nanotubes and Polymers. (August 2010)

Marion Odul Okoth, B.S., Minnesota State University-Mankato

Chair of Advisory Committee: Dr. Choongho Yu

This thesis describes the synthesis of a low modulus, thermally conductive thermal interface materials (TIM) using metal decorated nanotubes as fillers. TIMs are very important in electronics because they act as a thermally-conductive medium for thermal transfer between the interface of a heat sink and an electronic package. The performance of an electronic package decreases with increasing operating temperature, hence, there exists a need to create a TIM which has high thermal conduction to reduce the operating temperature.

The TIM in this study is made from metal decorated multi-walled carbon nanotubes (MWCNT) and Vinnapas®BP 600 polymer. The sample was functionalized using mild oxidative treatment with nitric acid (HNO_3) or, with N-Methly-2-Pyrrolidone (NMP). The metals used for this experiment were copper (Cu), tin (Sn), and nickel (Ni). The metal nanoparticles were seeded using functionalized MWCNTs as templates. Once seeded, the nanotubes and polymer composites were made with or without sodium dodecylbenzene sulfonate (SDBS), as a surfactant. Thermal conductivity (k)

measurement was carried out using ASTM D-5470 method at room temperature. This setup best models the working conditions of a TIM.

The TIM samples made for this study showed promise in their ability to have significant increase in thermal conduction while retaining the polymer's mechanical properties. The highest k value that was obtained was 0.72 W/m-K for a well dispersed aligned 5 wt% Ni@MWCNT sample. The Cu samples underperformed both Ni and Sn samples for the same synthesis conditions. This is because Cu nanoparticles were significantly larger than those of Ni and Sn. They were large enough to cause alloy scattering and too large to attach to the nanotubes. Addition of thermally-conductive fillers, such as exfoliated graphite, did not yield better k results as it sunk to the bottom during drying. The use of SDBS greatly increased the k values of the sample by reducing agglomeration. Increasing the amount of metal@MWCNT wt % in the sample had negative or no effect to the k values. Shear testing on the sample shows it adheres well to the surface when pressure is applied, yet it can be removed with ease.

DEDICATION

To my husband Ray Nelson, my parents, and my family.

ACKNOWLEDGMENTS

I would like to express my gratitude to all those who supported me while I completed this thesis. I am deeply indebted to my advisor Dr. Yu. Without his knowledge and assistance, this study would not have been successful. I would like to thank my family members, especially my husband Ray Nelson, and my parents for their emotional and financial support.

NOMENCLATURE

A	Surface area of the electronic component through which heat is emitted (m^2)
Ag	Silver metal
ASTM	American Society for Testing and Materials
^oC	Temperature in degrees Celsius
CNT	Carbon nanotubes
Cu	Copper metal
DAQ	Data acquisition
DBC	Direct bond copper
DI	Deionized
EDS	Energy dispersive spectroscopy
g	Mass in grams
h	Hour
H_2	Hydrogen gas
HNO_3	Nitric acid
IGBT	Insulated gate bipolar transistor
k_{TIM}	Thermal conductivity for thermal interface material (W/m-K)
k	Bulk thermal conductivity (W/m-K)
K	Temperature in Kelvins
min	Minute
MWCNT	Multi-walled carbon nanotubes

metal@MWCNT	Metal decorated multi-walled carbon nanotubes
Ni	Nickel metal
NMP	N-Methyl – 2 pyrrolidone
NP	Nanoparticle
NT	Nanotube
PCM	Phase-change materials
Q	Heat flow (W)
Q''	Power per unit area of the heat-emitting component (W/m^2)
R_{cond}	Thermal resistance across the thickness of the TIM (Km^2/W)
$R_{contact}$	Total thermal contact resistance (Km^2/W)
$R_{contact1}$	Thermal contact resistance for the electronic package (Km^2/W)
$R_{contact2}$	Thermal contact resistance for the heat sink (Km^2/W)
R_{int}	Effective thermal resistance of the interface (Km^2/W)
SDBS	Sodium dodecylbenzene sulfonate
SDS	Sodium dodecyl sulfate
Sn	Tin metal
SWCNT	Single-walled carbon nanotubes
T_g	Glass transition temperature (K,^oC)
t	Thickness of the thermal interface material (m)
T_{cpu}	CPU or other electronic package surface temperature (°C)
T_{hs}	Heat sink baseplate temperature (°C)
TEM	Transmission electron microscope

TIM	Thermal interface material
VACNF	Vertically aligned carbon nano fibers
VACNT	Vertically aligned carbon nanotubes
wt%	Weight percent

TABLE OF CONTENTS

CHAPTER Page

LIST OF FIGURES

FIGURE Page

LIST OF TABLES

CHAPTER I

INTRODUCTION

1.1 Thermal Interface Materials

Thermal interface materials (TIM) have gained a lot of prominence in recent years due to the increased demand for thermal management solutions for smaller and, more powerful electronic packages. Due to the decreasing size of current electronic packages (power devices and integrated circuits), thermal management is of great importance in trying keep these devices operating at optimal system specifications. For example, the typical heat generated by a 64-bit dual-core Intel Xeon® 7041 Processor running at 3.0 GHz clock speed is 165 W.[1] With such high heat generation, lowering the operating temperature becomes of utmost importance since the performance of transistors depends on it.[2] Higher operating temperatures increase the gate delay of transistors. This is compounded by the fact that devices now have more complex circuitry. With longer conducting paths due to complex circuitry, a longer gate delay time becomes a liability in the operating speed of the device. Also, increases in temperature in the presence of high humidity and an electrical potential could, induce electrical failure in the device.[2] The schematic of a typical insulated gate bipolar transistor (IGBT) package in an inverter with the direction of heat flow is shown in Figure 1. Thermal grease is used as the TIM and, a clamping pressure of around 0.17 to 0.34 MPa is used to keep the device in place.[3]

This thesis follows the style of Journal of Applied Physics.

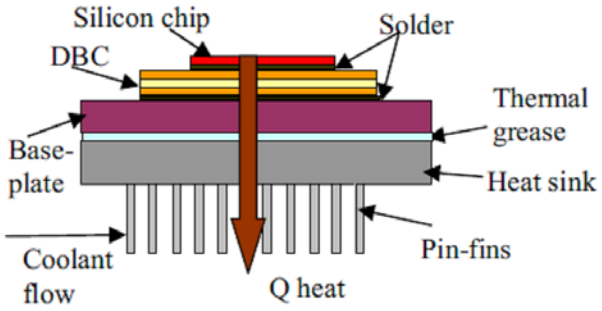

FIG.1. Schematic of IGBT electronic package showing direction of heat flow.[3]

There are many types of TIM products currently available. They range from Direct Solders, Greases, Phase Change Materials (PCM), filled Polymer Elastomers and Carbon based materials.[1] For example, Direct Solder attachment provides a high thermal conductivity in the range of 30-86 W/m-K. However, it is not an ideal interface material as the solder introduces thermal stresses, requires high temperature processing and, softer solders have poor mechanical properties.[1]

As the size of electronic package decreases, the dominant resistance in the interface shifts from the resistance within the interface material to the contact resistance as shown in Figure 2.

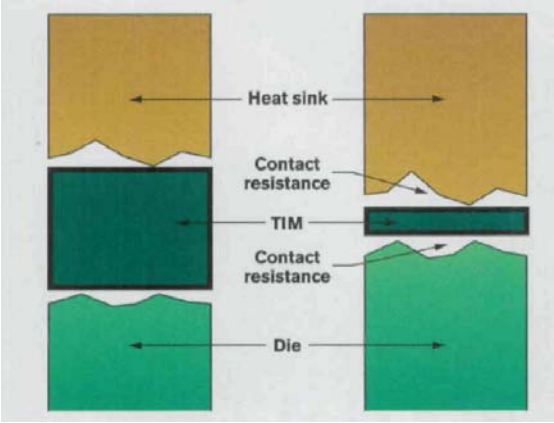

FIG.2. Dominant resistance in submicron interfaces.[2]

In order to improve the heat transfer without impeding mechanical properties, a material with a low modulus and, high thermal conductivity may be used to conform to the gaps in the interface as shown in Figure 3 (b).

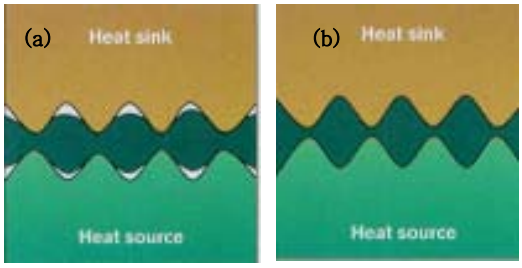

FIG.3. Wettability of (a) high modulus material and (b) low modulus material.[2]

Materials with better wetting capabilities fare better as TIMs at submicron and micron levels. As shown in Figure 4, the contact resistance is dominant since only a

small area of the contacting surfaces actually mates, leaving gaps that are filled with air.

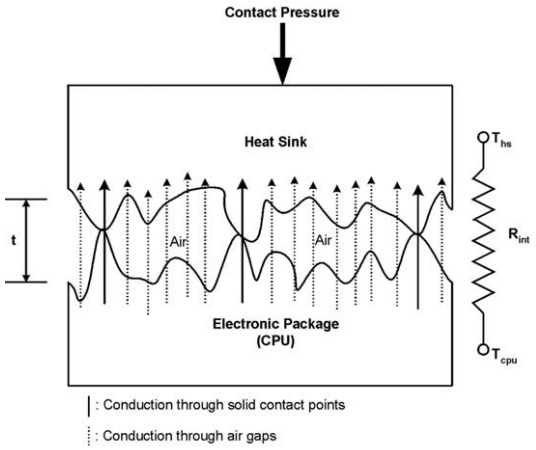

FIG. 4. Schematic of the thermal circuit of the interface showing air gaps.[5]

Since air is a poor thermal conductor (0.025 W/m-K),[4] it increases the thermal resistance in the interface. Some researchers have attempted to increase the mating area of the contacting surfaces by improving the surface finish of the heat sink. The result has only netted a paltry 2.5 % decrease in the thermal resistance.[1] The thermal resistances (R), in a typical thermal circuit of an interface are shown in Figure 5.

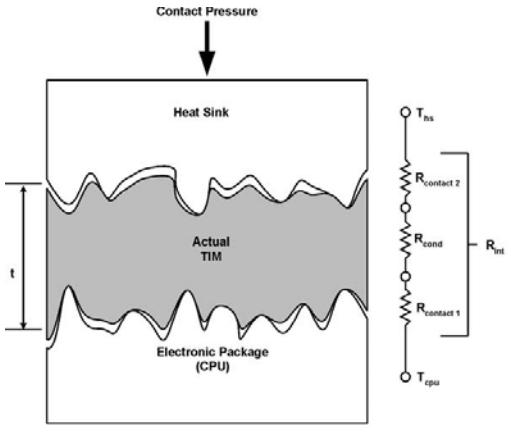

FIG. 5. Thermal resistance circuit for a typical interface.[5]

The equations to derive the effective thermal resistance (R_{int}), from the thermal circuit in Figure 5 at steady state are,

$$R_{int} = R_{contact1} + R_{cond} + R_{contact2} \quad (1)$$

$$R_{contact} = R_{contact1} + R_{contact2} \quad (2)$$

$$R_{cond} = \frac{t}{k_{TIM}} \quad (3)$$

$$R_{int} = R_{contact} + \frac{t}{k_{TIM}} \quad (4)$$

where t and k_{TIM} are the average bond line thickness of the interface and, the thermal conductivity of the interface material respectively. Hence, the most logical and cost effective means of reducing R_{int} without sacrificing material design considerations of the contacting surfaces is, to use a TIM with a high thermal conductivity and, a low modulus.

Greases are one such material as they are made by mixing a polymer base and a metallic or, ceramic filler. They usually have a very low modulus, are easily mounted

with low clamping pressures in addition to being cheap.[1] Their thermal conduction is generally not good but some state of the art greases such as Dow Corning® TC-5022 boast of having a k value of around 4 W/m-K.[3] The drawbacks to using greases other than their poor thermal conduction are, they are susceptible to drying out or being pumped out. This is due to contraction and expansion of the grease during thermal power cycles. This drying out or pumping out can impede product performance and cause contamination of other surfaces.[1] They are also messy, difficult to apply and, their degradation is dependent on the operating temperature and, the number of thermal cycles it undergoes.[5]

When selecting a TIM, it is also important to note that thermal conductivity and wettability are not the only factors that must be taken into account. Depending on the application, other factors such as, outgassing, surface finish, shear force, phase change temperature, clamping pressure, ease of application and, cost must be taken into account.

Outgassing or the release of gasses is a problem that adversely affects performance of TIMs. Polymer based materials outgas and this could create contamination problems within the package.[1]

The TIM must also have a low shear force so that it is easy to disengage in case the package has to be disassembled for repairs without breakage.

Phase change temperature (PCT), is also important to ensure that the TIM is able to operate at the maximum operating temperature and, won't melt during operation or shipping. PCT is the transition temperature between the solid and liquid phase of a material. At temperatures above PCT, the TIM will melt and pump out.[1] Phase change materials (PCMs), such as thermal pads, low melting alloys (LMAs) and, shape memory alloys are generally designed to have melting points below the maximum operating temperature.[1] They are solid at room temperature but melt and flow like grease when the electronic package is at its operating temperature. Their thermal resistances are comparable to that of greases whoever, polymeric based PCMs have higher thermal resistances than grease.[1] Unlike greases they don't have contamination issues, are easy to apply and, are not susceptible to drying out although, drip-out can be a problem for LMAs.[1] They also require higher clamping pressures than greases of upwards to 50 psi (344 kPa) which, is on the high end of what most chips can take.[5] Polymeric based PCMs have lower thermal conductivities but, they require constant pressure which introduces unnecessary mechanical stresses. LMAs are susceptible to oxidation and intermetallic growth.[1]

Thermally conductive elastomers consist of a silicone elastomer filled with thermally conductive particles.[1] They don't have the same wettability as greases and PCMs even at maximum operating temperature. They also have thermal resistances higher than greases.[1] For example, the Chomerics® THERM-A-GAP elastomer needs a clamping pressure of 70 kPa (10 psi) and has a thermal resistance between 3.9-10.3 ^{o}C

cm^2/W.[1] They also require a permanent clamping mechanism to maintain the joint which is a strong disadvantage for many applications.[1]

Polymeric based TIMs can also be made from Carbon based fillers such as exfoliated Graphite, Carbon nano-fibers and Carbon nanotubes (CNTs). Graphite has good thermal Conductivity 3000 $W\ m^{-1}\ K^{-1}$ and is cheap, making it a good candidate as a filler material.[6] For example flexible sheets of exfoliated Graphite impregnated with polymers have been found to have high thermal conductivities of about 5.7 W/m-K.[1] However, they do require high contact pressures more than any other interface materials for thicknesses greater than 0.13 mm.[1] Since exfoliated Graphite has poor solubility in water, it requires more complex fabrication methods that inhibit the cost effectiveness for mass production. The process of creating the exfoliated Graphite itself is complex.[6] Other carbon based fillers such as vertically aligned Carbon nano-fibers (VACNFs) have produced composites with good thermal resistance but, they require a very high clamping pressure of 414 kPa (60 psi).[1]

The mounting or clamping pressure plays an important role in the choice of a TIM. Most electronic packages cannot withstand high clamping pressures. For example a typical chip Intel P4 processor has a maximum allowable mounting pressure of about 0.116 MPa (16.78 psi).[5] Hence, the TIM must have a really low modulus in order to be able to deform easily under such low clamping pressures.

Carbon nanotubes are also good candidates for fillers in polymeric based TIMs. CNTs have gained a lot of prominence in the field of Nanotechnology since they were discovered by Ijima.[7] This is due to their high mechanical strength, good thermal and electrical conductivities. The thermal conductivity of individual CNTs is very high ranging from 6000-3000 W/m-K.[8] They have potential applications in fields such as electronics, material science, composites, biotechnology etc. They are also popular because they have potential to be mass produced in a cost effective manner.[9,10] There are two types of CNTs, single-walled carbon nanotubes (SWCNTs) and multi-walled carbon nanotubes (MWCNTs). SWCNTs are made of single graphite sheets forming a cylindrical tube whereas MWCNTs are made of concentric nanotubes.[9] SWCNTs are either semi-conductors or metallic depending on the direction the graphite is rolled.[9] Metallic SWCNTs and MWCNTs nanotubes have similar electronic transport properties. CNTs can be synthesized through carbon-arc discharge, laser ablation of carbon or chemical vapor deposition.[9] MWCNTs are more easily synthesized commercially, making them a cheaper alternative to SWCNTs.[10]

For the purpose of use in thermal management in composites, MWCNTs are preferred because they have inner layers that are not subjected to tube-tube interactions or, interactions with the polymer matrix.[11] These interactions as in the case with SWCNTs, have been known to create a permanent coupling with the polymer matrix which, causes phonon boundary scattering.[11] Hence, despite the high thermal conductivity of single tubes, CNT films see a rapid degradation in thermal properties.

Reported values of the thermal conductivity of CNT ropes, mats and, films range from 20 -200 W/m-K.[8] While that of CNT filled polymer composites ranged from 0.15 to 0.47 W/m-K which is much lower than that of single CNT tubes.[12] Degradation of thermal properties is mainly due to boundary scattering between tubes which is caused by the high amount of agglomeration between them as shown in Figure 6.

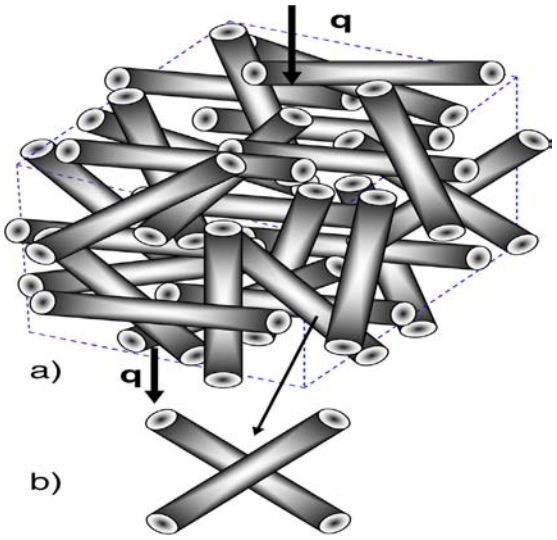

FIG. 6. Schematic of heat flow in CNT bundles showing agglomeration.[13]

Agglomeration in CNTs occurs due to the van der Waals attraction forces between nanotubes.[14] This affinity to agglomerate makes CNTs highly insoluble in common solvents such as water.[15] This makes them difficult to disperse them in the polymer matrix. Boundary phonon scattering can also occur between the polymer matrix and the tubes due to interfacial forces.[11]

Functionalization agents such as HNO_3 can cause oxidation of the NTs along their pristine sidewalls by, attaching groups of covalent molecules such as Hydroxyl, Carboxyl and, Carbonyl.[15] This makes the CNTs more hydrophilic and therefore easy to disperse in water. However, functionalization can reduce the CNT aspect ratio and, increase the interfacial interactions with the polymer.[16] Therefore, mild treatments are encouraged. Other agents such as N-Methly-2 Pyrrolidone (NMP), is also good for functionalization because it loosens the van der Waals forces but, it is also toxic.[17]

The use of surfactants can also reduce the amount of agglomeration. Two commonly used and readily available surfactants are, Sodium dodecyl sulfate (SDS) and, Sodium dodecylbenzene sulfonate (SDBS). They can be adsorbed on the surface of the funtionalized NTs. Studies done by Bystrzejewski et al. showed that SDBS has a 26-45% higher dispersing power than SDS.[14] The use of surfactants is a double edged sword since they also form supramolecular structures wrapped around the NTs making it harder for them to attach NPs and, they (supramolecular structures) increase interfacial phonon scattering.[12]

Alignment of CNTs in polymer films has been proven to be an effective method in reducing the tendency of CNTs to randomly agglomerate. Studies have shown that aligned SWCNT significantly reduced phonon-phonon Umklapp scattering. This encouraged phonon propagation in the axial direction of the aligned CNTs.[18] Vertically Aligned CNT (VACNT) films have also shown great promise in achieving unheard of k

values in CNT-polymer composites. Vertical alignment of the nanotubes is often achieved during the synthesis process.[19] This is done by growing them vertically using direct current during the synthesis process. Polymeric materials can then be injected around the vertically grown nanotubes to form the composite.[20] Huag et al. were able to double the thermal conductivity of polymer composite film from 0.59 W/m-K for normal dispersed CNT to 1.21 W/m-K for VACNT, for the same vol% of CNT.[20] The drawback to this method is that the synthesis method contains many complex processes such as growing the nanotubes vertically to begin with and, Reactive Ion Etching to reveal the CNT beneath the polymer veneer.[20] Large contact resistances between the surface and CNT have been observed in these films.[1]

Since functionalized CNTs contain defect sites, they can be readily used as a template to attach nanoparticles. Chen et al were able to grow Cu nanoparticles by dispersing CNT and a metal salt in a solvent.[21] The subsequent solution was filtered, dried and reduced in H_2 gas atmosphere. It is a simple, cost effective method which entails using the CNTs as a template to synthesize nanoparticles using only metal salts and, nanotubes as precursors.

The benefits of alignment can also be easily applied if highly magnetic metals are attached. The combination of magnetic alignment, surfactants, functionalization and, correct polymer choices can be used to achieve a good TIM which has a low modulus, is easy to manufacture, is cost effective and, has good mechanical properties.

1.2 Thermal Conductivity

As mentioned earlier the thermal conductivity of the TIM is very important. The total thermal conductivity (k), of a solid is composed of electronic thermal conductivity (k_e) and, phonon thermal conductivity (k_{ph}) as shown in equation 5.

$$k = k_e + k_{ph} \tag{5}$$

In metals k_e is dominant while in semiconductors k_{ph} is dominant. The thermal conductivity of nanotubes at room temperature or higher, is dominated by phonons.[22] According to the kinetic theory, the phonon thermal conductivity is given by,

$$k_{ph} = \frac{1}{3} cvl \tag{6}$$

where is c the specific heat capacity, v is the lattice vibration velocity of phonons and, l is the phonon mean free path.[23] When the temperatures increases, the mean free path l decreases.[24] The mean free path of a phonon is found using Matthiessen's rule as shown in equation 7 below as,

$$\frac{1}{l_{ph}} = \frac{1}{l_{defect}} + \frac{1}{l_{phonon}} + \frac{1}{l_{boundary}} \tag{7}$$

where l_{defect}, $l_{interface}$ and $l_{boundary}$ are the phonon mean free path of phonon due to defect scattering, phonon-phonon Umklapp scattering and, phonon boundary scattering respectively. In CNT bundles or ropes, phonon-phonon Umklapp scattering is severely suppressed therefore the dominant form of phonon scattering is at the boundary.[22] Hence tube-tube interactions play a very important role in the thermal conduction due to their influence on the mean free path.[22] In a polymer composite, phonon conduction is also dependent on the interactive forces between the filler material and, the polymer matrix.[11]

These interactive forces can cause a large thermal resistance to exist across the nanotube-polymer matrix interface.[25]

The thermal conductivity for the TIM is best measured using ASTM D-5470 method at steady state. This is because most TIMs have temperature sensitive thermal properties and, it closely models the working environment in the electronic package.[5] The ASTM D-5470 test stand consists of two copper blocks attached to steel rods which are insulated. Heat flows through the setup from the heated copper block to the cooled one through the connected Steel rods. The sample to be measured is squeezed at the mid-point of the Steel rods as shown in Figure 7. The temperature gradient of both Steel rods can be found by first graphing the measured steady state temperature recorded by the thermocouples as a function of position.

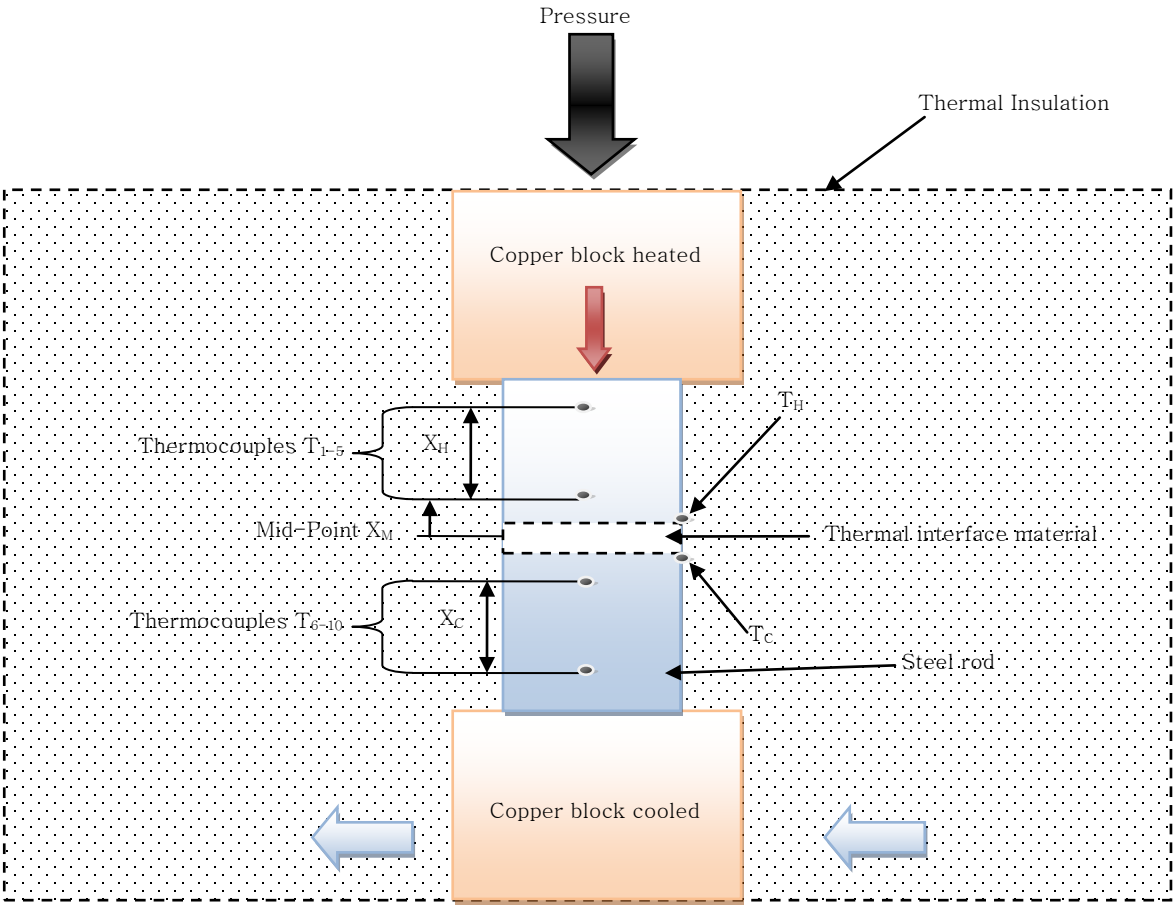

FIG. 7. Schematic of the experimental setup for ASTM D-5470.

Linear Extrapolation of these plots can then be used to find the temperature gradient of the heated and cooled sides across the rod as shown in Figure 8.

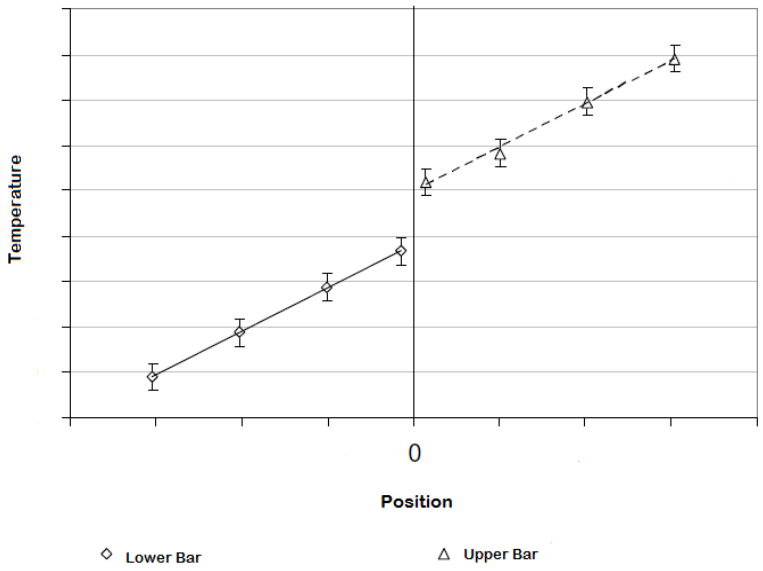

FIG. 8. Temperature gradient across the steel rod as a function of position.

Once this gradient is known, it can be used to find the theoretical temperature difference across the sample to be measured. This temperature is referred to as the Junction temperature and, is the temperature difference between the heated and cooled sides of the sample. The temperature on both the heated (T_H)and, cooled sides (T_C), at the median position x_M as shown in Figure 7, is found using equations 8 and 9.

$$T_H = T_5 - \frac{x_M\left(T_1 - T_5\right)}{x_H} \tag{8}$$

$$T_C = T_5 + \frac{x_M\left(T_6 - T_{10}\right)}{x_C} \tag{9}$$

The heat flow through the Steel rod should ideally be the same. However, due to experimental heat loss to the atmosphere, the heat flow through the Steel rod will vary

between the heated and, the cooled sides. The heat flow through each Steel rod shown in Figure 7, is found using Fourier's Law as shown in equations 10 and 11 where,

$$Q_H = k_{steel} A_{rod} \frac{(T_1 - T_5)}{x_H} \tag{10}$$

$$Q_C = k_{steel} A_{rod} \frac{(T_{10} - T_6)}{x_C} \tag{11}$$

k is the thermal conductivity of the steel rod, A is the cross-sectional area, T is the temperature measured at each specific point and, x is the total distance along which the temperature measurements are taken for the heated and, the cooled sides.

Thermal Conductivity of the interface material k_{TIM} can then be found with Fourier's law. This is done using the average of the heat flows found using equation 10-11, the Junction temperature difference and, the thickness of the sample as shown in equation 12.

$$k_{TIM} = \left(\frac{Q_H + Q_C}{2}\right)\left(\frac{t}{A(T_H - T_C)}\right) \tag{12}$$

1.3 Shear Stress Measurement

The shearing force is the force applied on the TIM parallel to the surface. This is usually applied when the joint is being disassembled or, when the electronic package or the heat sink is in horizontal motion. The maximum shear stress in the interface due to the bond is important due to the delicate nature of electronic packages. They are very brittle and, susceptible to breakage especially when it comes to time disengage them. A simple shear test measurement apparatus can be modeled using two contacting surfaces

to simulate a heat sink and an electronic package. The heat sink is usually a metal with a high k value such as copper or aluminum while, an electronic package can be simulated with a piece of Silicon film since most packages are made from Silicon dies. The simplified setup is shown in Figure 9.

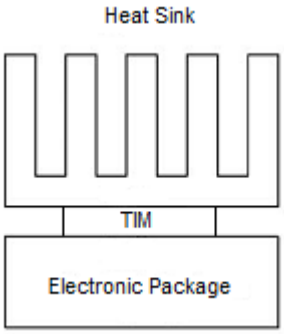

FIG. 9. Simplified schematic showing heat sink and electronic package.

CHAPTER II

SAMPLE PREPARATION, THERMAL CONDUCTIVITY AND SHEAR STRESS MEASUREMENT

2.1 Nanotube Functionalization

The as-received MWCNT's from Cheap Tubes Inc were functionalized using a mild oxidative acid treatment. The acid used was 70 wt % HNO_3 from Fisher Scientific. The ratio of MWCNT to HNO_3 was 2.5 g for every 50 ml of acid. The mixture was then sonicated in a Branson 1510 Ultra Sonic bath sonicator for 5 min and, magnetically stirred at around 80^oC for 4 h on a hot plate. After that, the nanotubes were vacuum filtered and washed repeatedly with DI water to remove all traces of the acid. The purified MWCNT were then left to air dry.

Functionalization was also done with N-Methyl-2 Pyrrolidone (NMP), from Fisher Scientific. The as-received nanotubes were left to soak overnight in a beaker full of NMP solution at room temperature. The solution was then filtered and soaked with Heptane from Fisher Scientific, overnight while stirred. It was then rinsed multiple times with DI water and allowed to dry at room temperature.

2.2 Metal Decoration of Nanotubes

Once the nanotubes were dried, they were ready for metal decoration. The method used to decorate them was first developed by Chen et al.[21] However, it was altered for the purpose of this experiment through trial and error. Various metal to nanotube ratios

were made to show the effects of increasing the amount of metal in the composite. The different metal nanoparticles that were synthesized were Cu, Sn and, Ni. The metal salts used were $CuSO_4$, Ni $(NO_3)_2$ from Fisher Scientific and, $SnCl_4$ from Alfa Aesar. The amount of the metal salt added was based on the ratio of the metal to CNT.

The purified nanotubes were first sonicated in a beaker full of DI water for 10 minutes to partially disperse them. Subsequently, the metal salt was added into the beaker and sonicated for an additional 10 minutes, to aid in the dissolution. Once the salt was dissolved, the mixture was magnetically stirred on a hotplate at 80^{o}C for 24 h. The metal decorated nanotubes were then filtered to remove excess solution and dried in air. Once dried, the metal@MWCNT composite was reduced in a H_2 gas atmosphere in an airtight tube furnace at 150 ^{o}C for 6 h.

2.3 Sample Preparation

To prepare the sample, the total dry mass of the composite was determined. This usually ranged from 0.6 g to 1.0 g depending on the desired thickness of the sample. It is important to quantify this since, the amount of filler materials that can be added to make a film is limited. This range was found by trial and error. The maximum amount that can be added to make a film is 60 wt%. Thicker samples are easier to remove hence were preferred but, a thickness of around 0.2 mm is desired for this type of application thereby limiting the thickness. The dried metal@MWCNT composite or the functionalized MWCNT for the reference samples were weighed depending on the desired weight

percent. The metal @MWCNT wt% used for this study was 4, 5, 10, 25, and, 40. This was mixed in with or without surfactants such as SDBS from Fisher Scientific. SDBS was added until the nanotubes looked visually dispersed. This mass was noted and, the wt% of SDBS was calculated from the final dry mass tally. Other filler materials such as Exfoliated Graphite from Mc-Master-Carr were also used in some samples. Once the dry filler materials were mixed into a plastic bottle, water was added and, the mixture was sonicated using a MISONIX XL-200 Pen Tip Sonicator as shown in the Figure 10.

FIG. 10. Sonication apparatus.

The polymer used for this study was Vinnapas® BP 600 emulsion from Wacker

Chemicals which has a 55.16 solid wt%. It has a glass transition temperature (T_g), of -40^{o}C and a thermal conductivity of 0.13-0.14 W/m-K. The weight of the polymer emulsion was then determined by finding the dry mass of the polymer to be added and, dividing it by the solid weight percent of the emulsion as shown in equation 13.

$$W_{\text{Polymer emulsion weight}} = (W_{\text{Total dry}} - W_{\text{metal@MWCNT}} - W_{\text{surfactant}} - W_{\text{filler}})/.5516 \quad (13)$$

The total amount of water used was no more than 20 g which was found by trial and error. This was to ensure faster drying times, adequate liquid to disperse the nanotubes and, adequate liquid so as not to cause surface blistering of the film upon drying. Once the composite was properly sonicated, the films were then cast onto a plastic container as shown below in Figure 11(a).

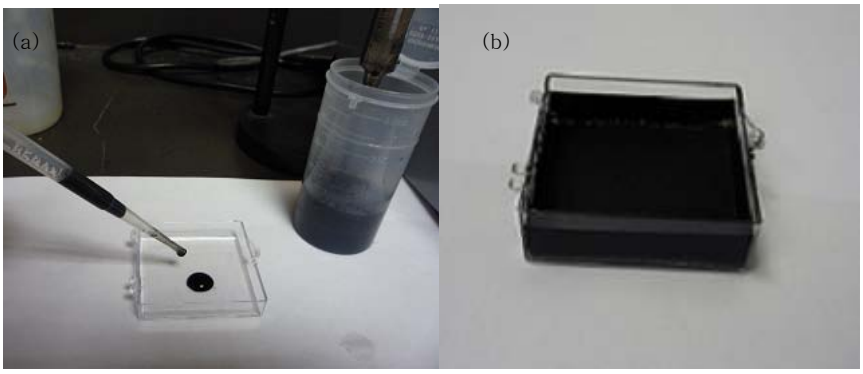

FIG. 11. (a) Film casting and (b) finished film.

They were then left to air dry in a fume hood to almost 60 %. Films that were to be

aligned were allowed to air dry in a magnetic field. This usually took about 2 days. Then, they were removed and cured in an oven at 80^{o}C for 1 h. A sample of the finished film is shown in Figure 11 (b).

2.4 Thermal Conductivity Experimental Setup

The ASTM D-5470 steady state method was used to measure the thermal conductivity. The measurement apparatus shown in Figure 12, consists of two copper blocks across which heat is transferred thorough two attached Steel rods as shown in Figure 12 (a). The lower block is cooled by a refrigerant and the upper one is heated by heater. Pressure was also applied to the sample by adding a load to the top of the setup as shown in Figure 12 (b). Equidistant thermocouples are attached to the Steel rods to make thermal measurements as shown in Figure 12 (a). The thermocouple measurements were recorded using Lab View programming via a DAQ board.

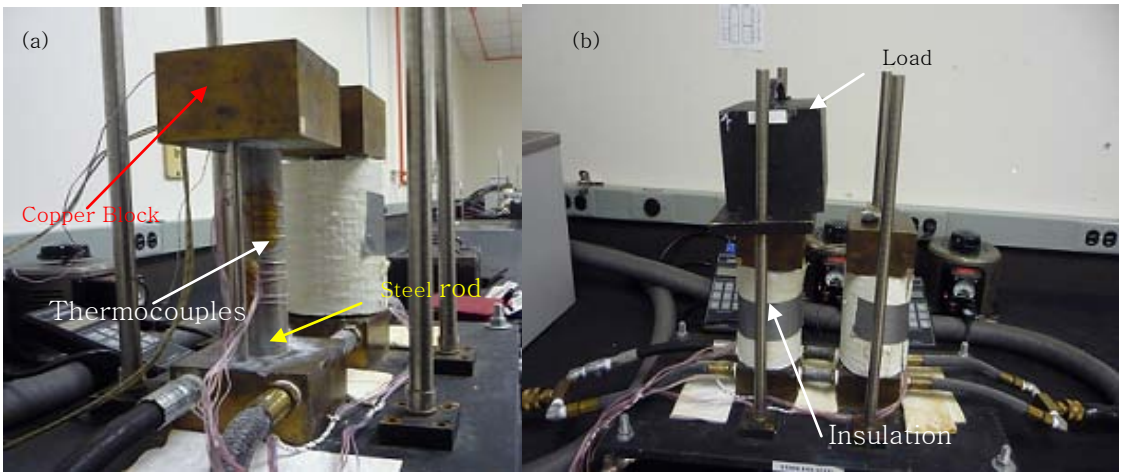

FIG.12. The experimental setup for thermal conductivity measurement (a) showing thermocouples (b) with insulation and the load on.

Once the heater and refrigerant reached their set steady state temperature of 50^{o}C and 0^{o}C respectively, Silicone® thermal paste was applied to interface of the steel rods. The system was allowed to go back to steady state. The first run was to get the thermal resistance contribution of the Silicone® paste. When the temperature reached steady state, a 1 mm^{2} in area circular sample was added onto the interface between the heated and cooled Steel rods. The setup was allowed to reach steady state again in order to collect temperature measurements data for the sample. The thermal conductivity was then calculated using equations 8-12 subtracting the Junction temperature contribution of the Silicone® paste. This procedure was repeated for all the samples.

2.5 Shear Stress Experimental Setup

For the shear stress experiment a sample holder made from Aluminum was

fashioned to simulate a cold sink and silicon die interface. Since Tensile testing was to be performed, the sample holders had to be coaxial so an L-Shaped joint was cut on both pieces to make them mate as shown in Figure 13 (b). A depression was milled into it one of the pieces to hold a piece of Silicon film with epoxy as shown in Figure 13 (a). A piece of dried cured film which had the best k value (5 wt% Ni@MWCNT, 25wt% SDBS) was cut off the cast. It was then loaded onto the sample holder as shown in the Figure 13 (a).

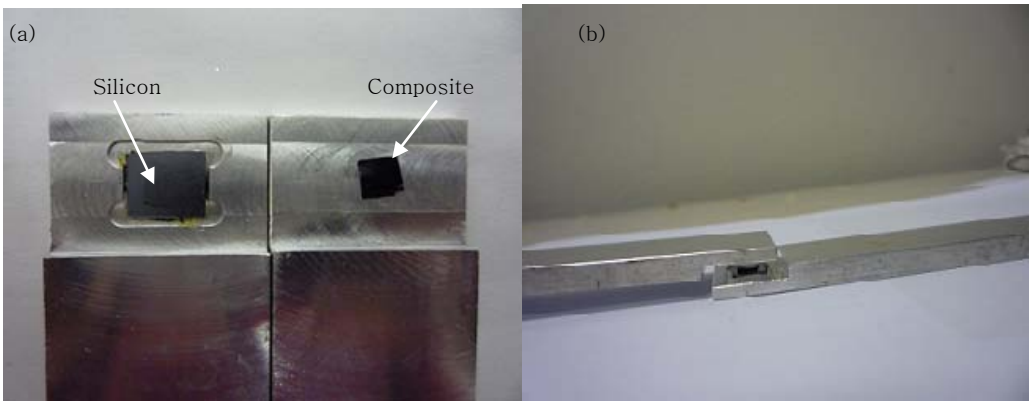

FIG. 13. Shear stress sample holder (a) initial sample (b) assembly.

The bond between the two contacting surfaces was formed by either hot or cold pressing. The hot pressing was done in a Specac Hydraulic Press at a temperature of 100 ^{o}C with a force of 50 kg as shown in Figure 14 (a). The cold pressing was done using a Carver Laboratory Press shown in Figure below 14 (b) with a force of 1 and 3 tons.

FIG.14. (a) Hot press and (b) cold press.

After hot pressing the sample was then loaded onto an INSTRON 4411 Tensile test machine as shown below in Figure 15, to simulate shear forces acting parallel to the bond.

FIG. 15. Tensile test apparatus.

Once the test was done, the force at separation was noted and this was taken to be the shear force. For the cold pressed test sample no tensile test was done as no formidable bond was formed between the two contacting surfaces. Further testing was done this time using minimal amount of force and heat. The sample was loaded onto an oven heated to 72^{o}C with a 100 g weight untill it became hot. The assembly is shown in Figure 16.

FIG. 16. Test sample with minimal force and temperature.

2.6 Sample Characterization

The metal decorated nanotubes were analyzed using a JEOL 2010 Transmission Electron Microscope (TEM). Energy Dispersive Spectroscopy analysis (EDS), was also performed on the TEM samples to find the chemical composition of the nanoparticles with the same apparatus.

2.7 Error Analysis

Error analysis was done on the thermal conductivity values by estimating the uncertainty in the values. This was done by finding the standard deviation of the sample population of the k values using equation 13 below.

$$S_X = \left[\frac{1}{N-1} \sum_{i=1}^{N} (x_i - \overline{x})^2 \right]^{\frac{1}{2}} \tag{13}$$

CHAPTER III

THERMAL CONDUCTIVITY OF CARBON NANOTUBE AND POLYMER COMPOSITES

3.1 Results

The image result of the metal decorated MWCNTs are shown below in Figures 17-19. Tables 1-3 show the EDS analysis of the TEM images of Figures 17-19.

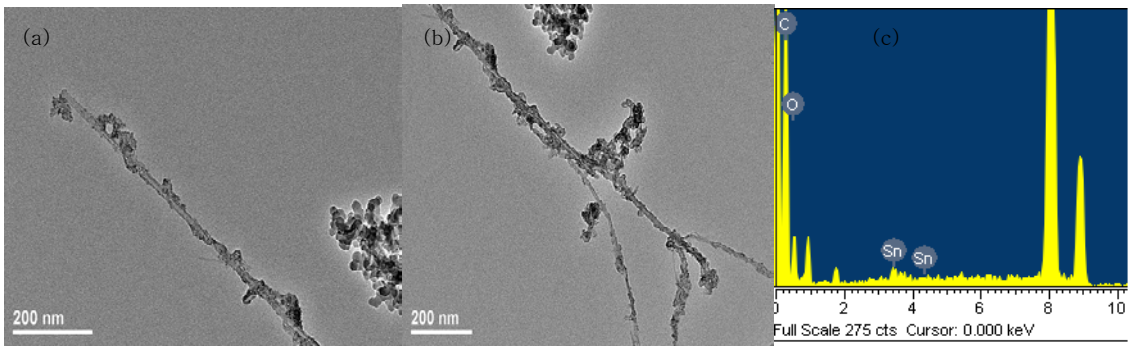

FIG. 17. TEM images of single Sn@MWCNT
(a) top (b) bottom (c) EDS of image (b).

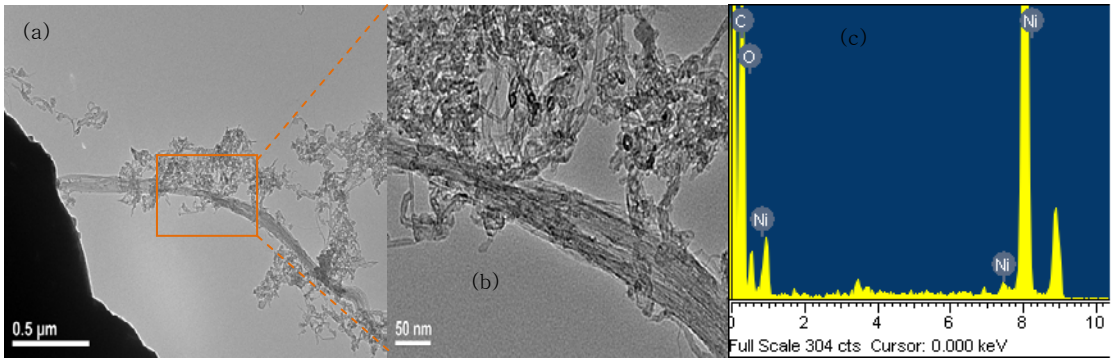

FIG. 18. TEM images Ni@ MWCNT ratio 2:1 (a) low magnification (b) high magnification image (c) EDS of image (a).

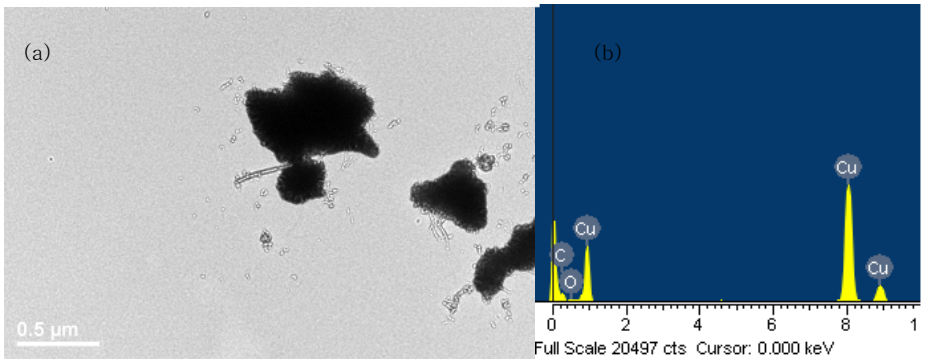

FIG. 19. (a) TEM image showing Cu@MWCNT with a metal to NT ratio of 2:1 (b) EDS of image (a).

Table 1 EDS analysis Sn@MWCNT.

Element	Weight%	Atomic%
C	88.39	94.08
O	6.75	5.39
Sn	4.86	0.52

Table 2 EDS analysis Ni@MWCNT.

Element	Weight%	Atomic%
C	94.08	95.95
O	5.05	3.86
Ni	0.87	0.18

Table 3 EDS analysis Cu@MWCNT.

Element	Weight%	Atomic%
C	2.60	12.22
O	0.54	1.89
Cu	96.86	85.89

The thermal conductivity measurements are shown in Figures 20-24. Tables A1-A6 in the Appendix A lists all the samples that were successfully made for this study. Where two values of thickness are listed, it indicates that two samples were cut from the same cast and measured for comparison. The results of the thermal conductivity measurements and error analysis are displayed in Table B1 in Appendix B.

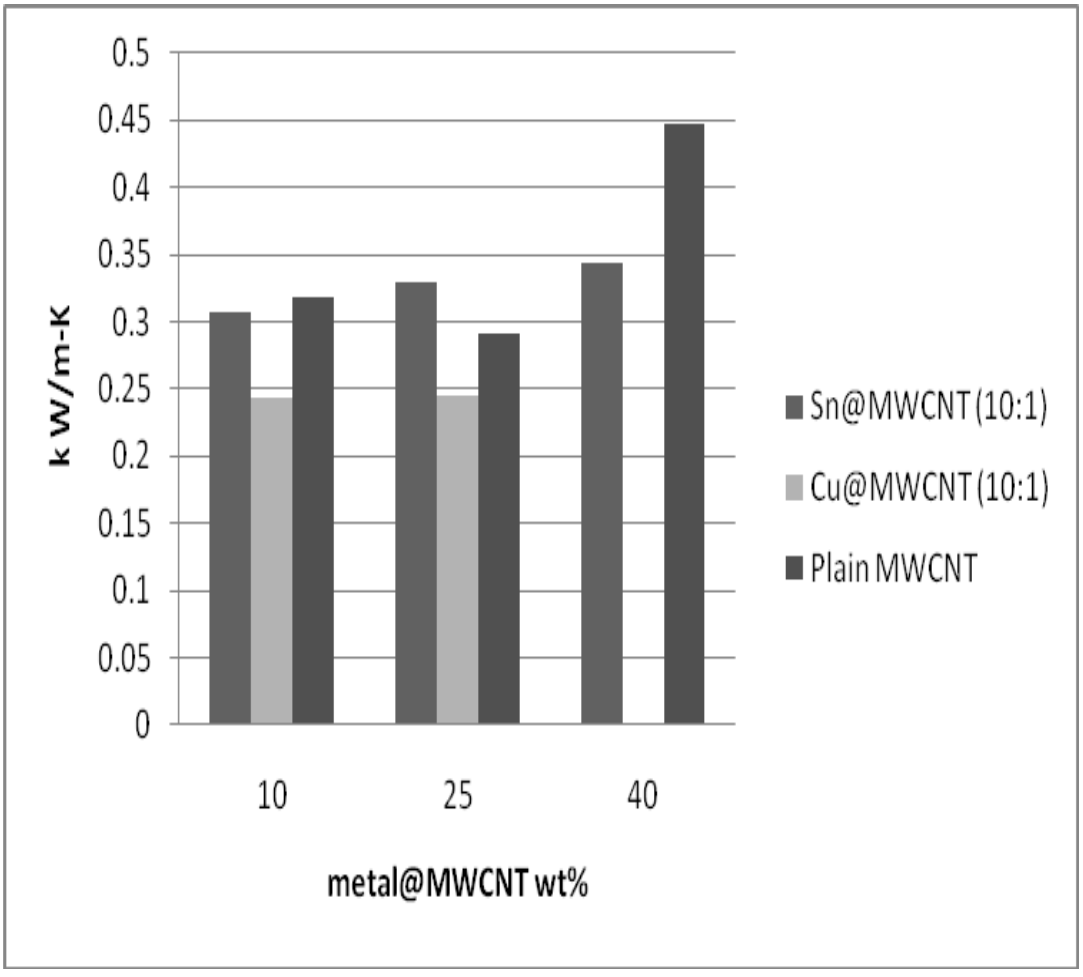

FIG. 20. Comparisons between k values of plain, Sn and Cu decorated CNTs.

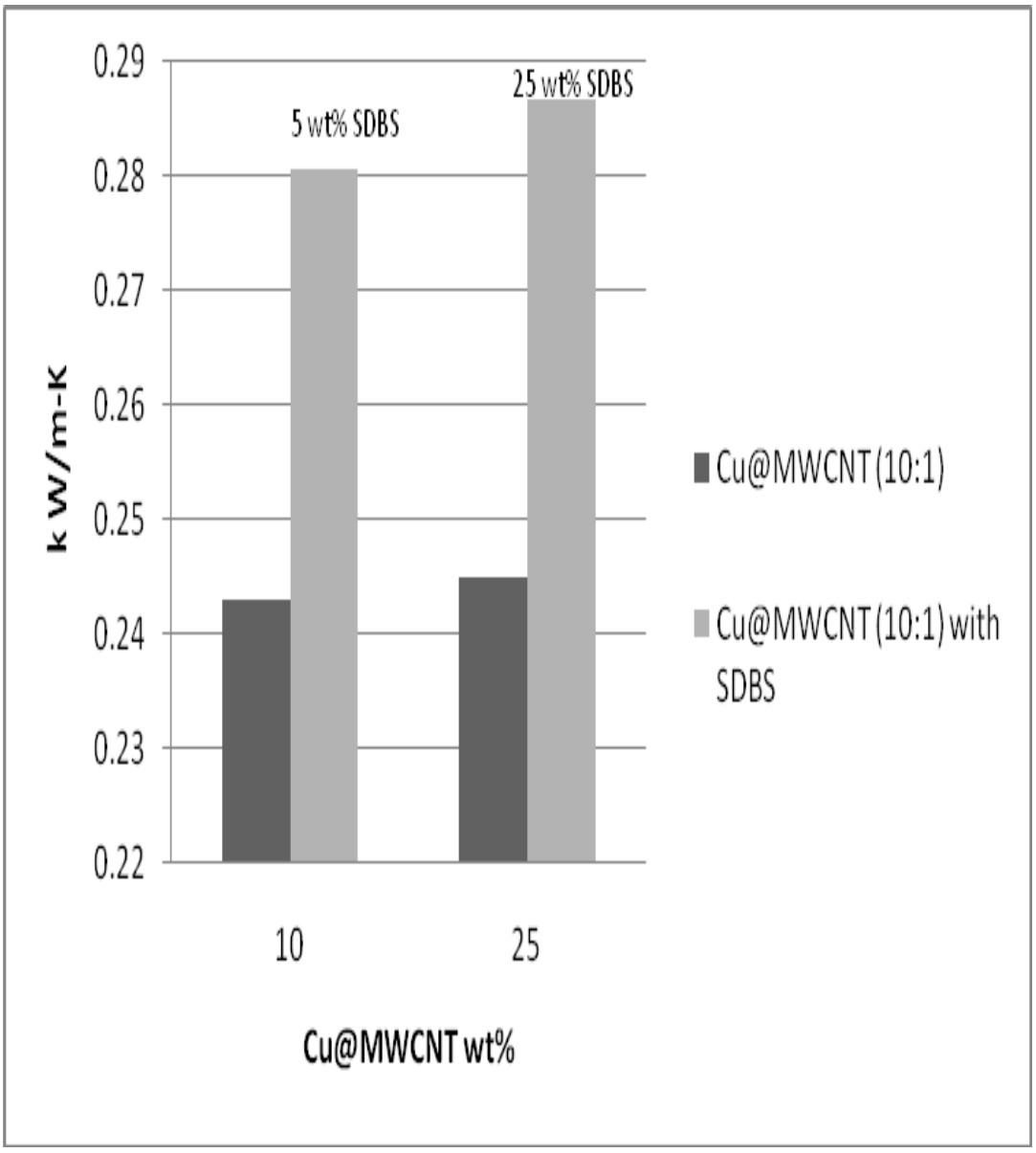

FIG. 21. The effect of surfactant on k value.

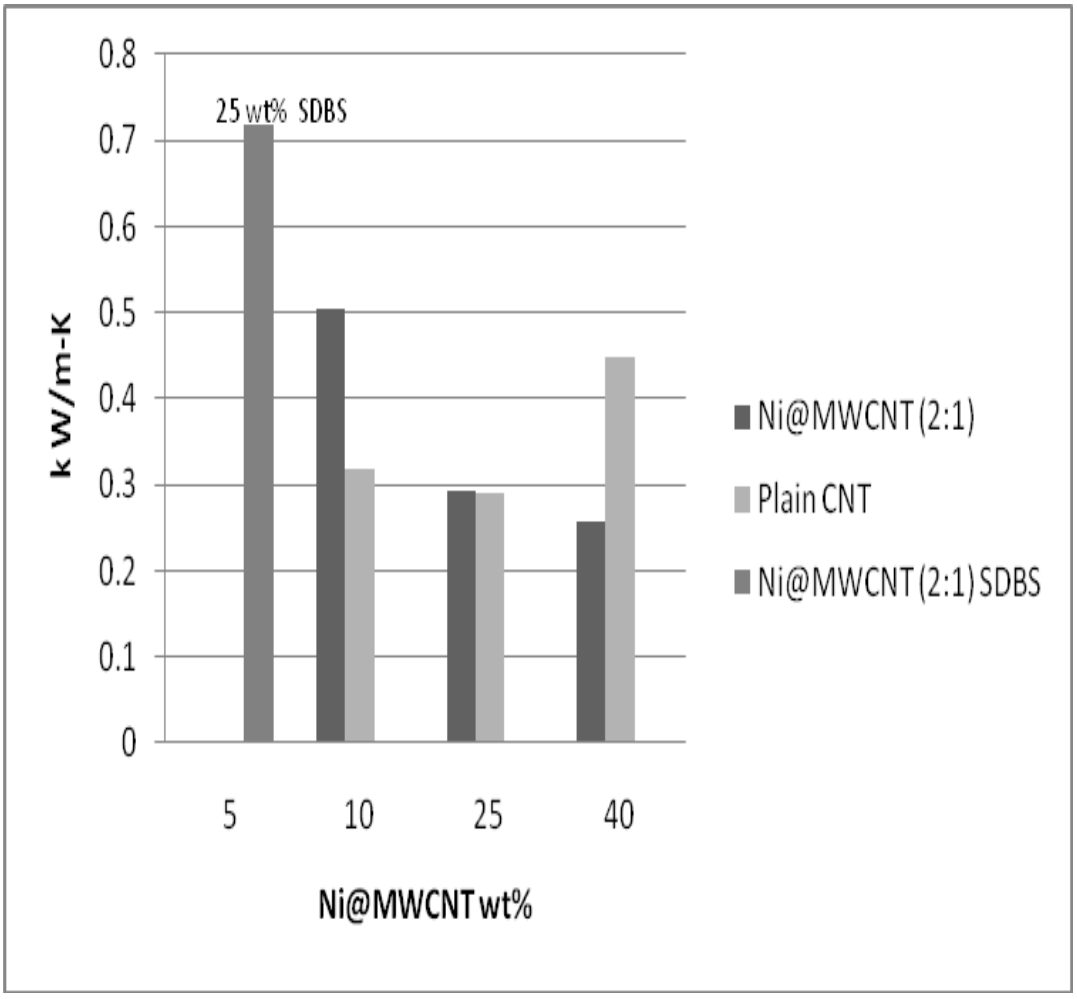

FIG. 22. Trends in k value for magnetically aligned Ni@MWCNT films.

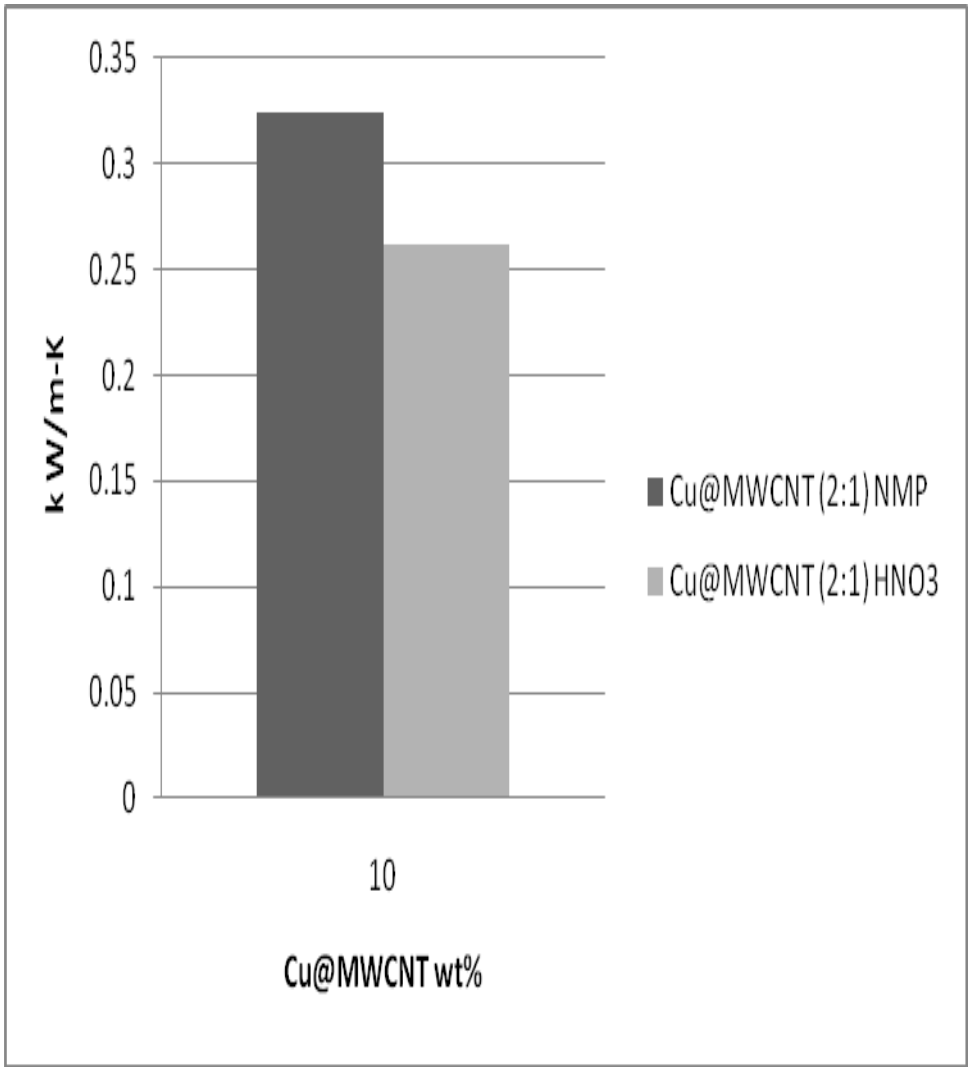

FIG. 23. Effect of using different functionalization agents.

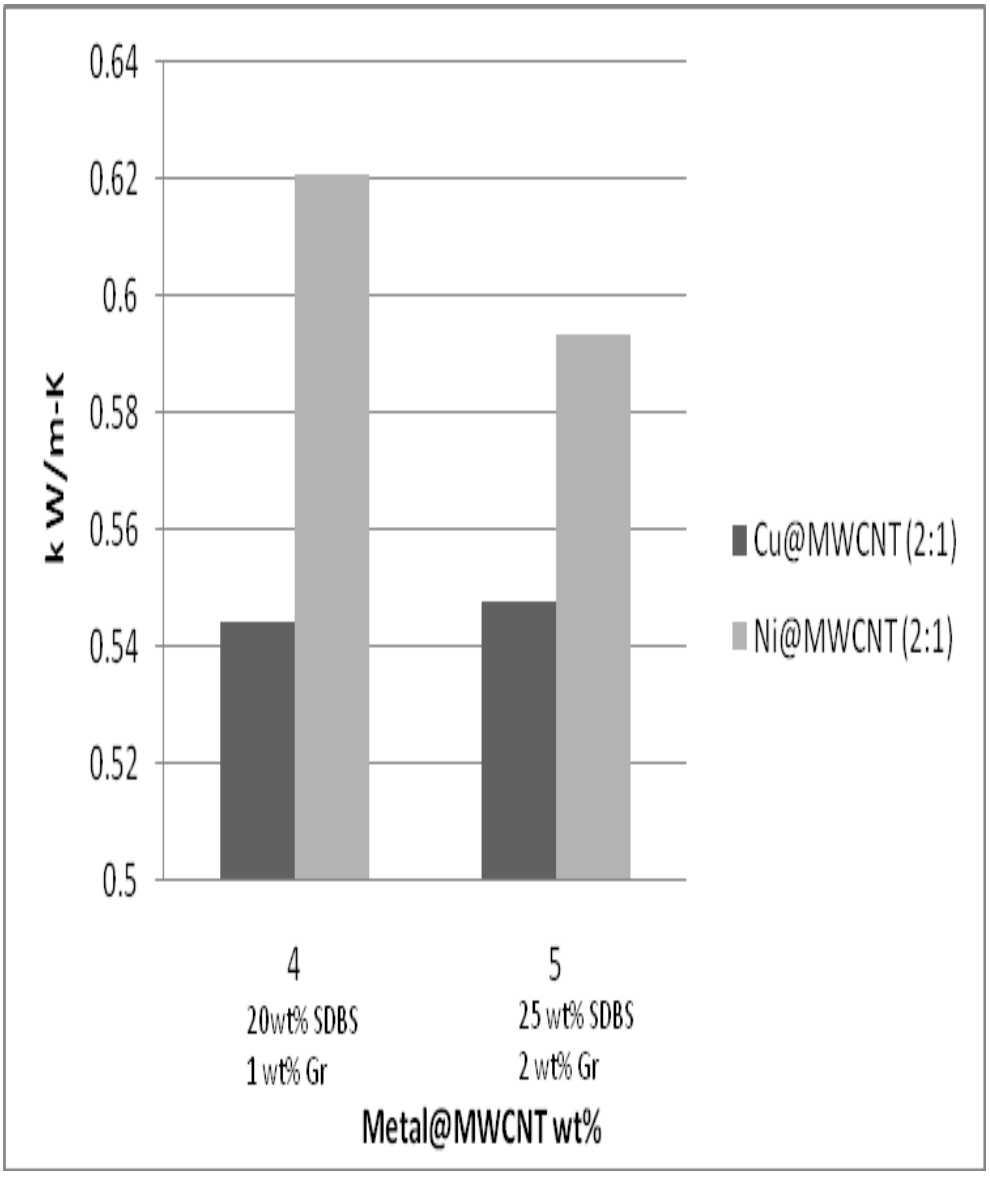

FIG. 24. Effect of using exfoliated graphite as an additional filler material on magnetically aligned samples.

The test samples for shear testing are shown in Figures 25-26.

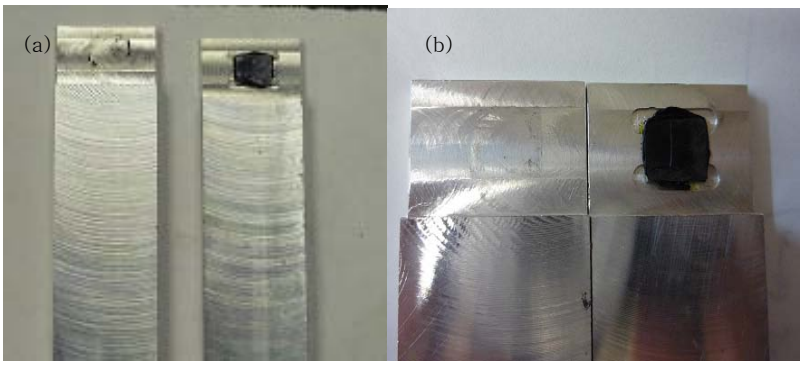

FIG. 25. (a) Hot pressed sample after tensile test (b) cold pressed sample after pressing.

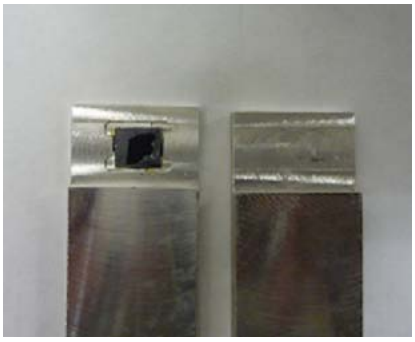

FIG. 26. Test sample after pressing with minimal force and temperature.

3.2 Discussion

Based on the EDS analyses, there is a small weight ratio of metal to O_2 in the metal@MWCNT composite as shown in Tables 1 and 2. As there is oxygen naturally in the TEM chamber, this may be indicative of that and not of a metal oxide being present. The EDS analysis in Table 3 could not provide definitive information on the atomic and weight % as Cu grids were used for the TEM. The lack of other constituent elements

from the metal salts in the EDS analyses presented in Tables 1-3, seems to indicate that the Hydrogen reduction process was successful**.** From the TEM images in Figures 17-18, actual metal nanoparticles are attached to the nanotubes. The metal particles for Cu are the largest followed as shown in Figure 19, then followed by Sn and Ni respectively. The metal particles in the Sn and Ni samples are really small (in nm range) and, not a lot which seems to suggest very little of the metal was attached despite increasing metal to nanotube ratio.

From the thermal conductivity measurements, the highest value was 0.72 W/m-K from the 5 wt% Ni@MWCNT which (dispersed with 25 wt% SDBS) sample, as shown in Figure 22. This is almost 7 times that of the neat polymer which around 0.13 -0.14 W/m-K and, 3 times of reported k values of plain CNT composites measured at room temperature for the same weight percent.[11] Yet, as impressive as this sounds, it is still low for a TIM with such high wettability such as greases.[1] Ma et al. were able to get a k value of 0.9 W/m-K for a 0.5wt % Ag@ SWCNT- polymer composite.[16] Even though this k value is slightly higher than what is found in this study, the method of composite fabrication they used was more complex than the one used here. They also used a Flash Laser to measure k which is a transient testing method. Due to the temperature sensitive properties of a TIM, only steady state testing methods are recommended to accurately gauge thermal conduction. They also used Silver (Ag) metal which, has a higher k value (429 W/m-K)[16] than the metals used in this study but, is very expensive.

Studies have shown that aligned nanotubes allow for better propagation along the axial direction of the nanotube.[18] Even though Cu metal has one of the highest k values for bulk materials (401 W/m-K), it's magnetically aligned composites performed poorly as shown in Figure 24, against Ni which has a lower bulk k value (90.7 W/m-K).[4] This is because Ni has better magnetic properties and, was therefore more easily aligned in the magnetic field. The Cu composites k values were also comparable to but, slightly less than those of Sn as shown in Figure 20. This is despite the fact that Sn has a lower bulk k value of 66.6 W/m-K compared to that of Cu (401 W/m-K).[4] The k values of Sn and Cu composites were both less than 0.35 W/m-K which is low for TIMs. From the TEM images, large growths of Cu nanoparticles was observed in Figure 19. Although phonon boundary scattering is a major factor in nanotubes, defect or alloy scattering is also important in nanoscale thermal transport. The Cu particles also failed to attach to the MWCNTs as they were too large as shown in Figure 19. Sn however, had better nanoparticle attachment than Cu as shown in Figure 17. In the plain functionalized nanotube composites, the only inhibitor of thermal conductivity is the interface thermal resistance. With metal@MWCNT, the effects metallic attachments have on the thermal resistance also have to be taken into account. This may explain why the Cu samples consistently underperformed both Sn and Ni for the same synthesis conditions.

Increasing the amount of CNT also didn't improve the k value for the metal decorated samples as shown in Figures 20 and 22. In general, the plain functionalized CNT samples had better k values at higher CNT wt% than the metal decorated ones.

This is due to secondary agglomeration and the inability to properly disperse the CNTs in the sample as the filler content increased.[16] At higher Ni@MWCNT wt% , the k values were lower than those of the plain functionalized CNT composites as shown in Figure 22.

Functionalization agents such as NMP and HNO_3 appeared to have the same effect on the k value as shown in Figure 22. However for this method HNO_3 is preferred because it is less toxic and, the functionalization process is less time consuming. The use of surfactants proved invaluable in increasing the thermal conductivity as shown in Figures 21 and 22. With better dispersion there is less agglomeration hence, there is less phonon boundary scattering that is brought on by tube-tube and, polymer-tube interactions. Also, a lower metal@MWCNT weight % allows for easier dispersion. As shown in Figure 24, increasing the filler material despite an increase in surfactant still could not increase the thermal conductivity. Among the magnetically aligned Ni samples shown in Figure 22, those that were dispersed with SDBS had better k values and, the k values decreased with increasing Ni@MWCNT wt%. The addition of exfoliated Graphite to the sample did not make it more thermally conductive. This is due to the fact that most of the exfoliated Graphite was denser than the other composite materials and, sunk to the bottom of the film during drying despite being well dispersed.

The shear stress was also successful in proving that this material can easily be applied and taken apart. A shearing force of less than one hundredth of a lb was found

for the hot pressed sample. The cold pressed sample could be taken apart by hand. Similarly, the sample pressed at 100^{o}C with a weight of 100 g, could be also be taken apart by hand without much force.The sample was also able to deform significantly as shown in the before and after pictures of the test specimen shown in Figures 25 and 26. This shows that in spite of an increase in filler material, the sample still retains a low modulus due to the low T_g of the polymer. It is also easy to cut into desired shapes.

CHAPTER IV

CONCLUSION

This thesis describes the methods and materials used to develop a polymeric based TIM with metal decorated MWCNT as fillers. Additional fillers such as exfoliated Graphite are also explored. The MWCNTs were functionalized with either 70 wt % HNO_3 or, NMP. Functionalization with HNO_3 was done by partially dispersing MWCNT in HNO_3 solution in the ratio 2.5 g nanotubes for every 50 ml of acid. The mixture was then magnetically stirred on a hot plate at a temperature of 80^oC for 4h. After that, it was filtered, rinsed with DI and, air dried. NMP functionalization was done by soaking MWCNTs overnight in a beaker full of the solution. The solution was then filtered, and soaked in a beaker full of Heptane solution overnight. It was subsequently filtered, rinsed with DI water to remove all traces and, air dried. The metals used to decorate the nanotubes were Sn, Cu and Ni. The metal decoration was done by mixing functionalized nanotubes with constituent metal salts. The metal salts used for this study were $CuSO_4$, Ni $(NO_3)_2$ and $SnCl_4$. The composites were then left to dry in air with some being aligned in a magnetic field during the drying process.

The thermal conductivity, for the metal decorated CNT-polymer composites was measured using the ASTM D-5470 method at steady state. The highest k value achieved in this study was 0.72 W/m-K for the 5 wt% Ni@MWCNT dispersed with 25 wt % SDBS sample. This value was almost 7 times that of the neat polymer (0.13-0.14 W/m-

K) and, almost 3 times of reported values of plain CNT composites at room temperature, for the same weight percent. Among the magnetically aligned Ni samples those that were not dispersed using surfactants had decreasing thermal conductivity with increasing metal@MWCNT wt%. Alignment seemed to favor Ni decorated samples over Cu as they had better higher k values as shown in Figure 24, for the same surfactant and filler amount. Also, Sn decorated CNTs had slightly better k values than Cu even though Cu has a higher bulk thermal conductivity as shown in Figure 20. Their k values were however no more than 0.35 W/m-K which is low for the purposes of TIM. This is because as observed in the TEM images, the Cu particles were significantly larger than the Sn and Ni ones. This may have contributed to alloy/defect scattering of the phonons in the sample. Also, due to their size they were unable to attach to the MWCNT. The type of functionalization agent used had little or no effect on improving the k values as shown in Figure 23. Overall, thermal conductivity either decreased or remained the same with increasing CNT wt%. There was no benefit to increasing amounts of CNT as shown in Figure 22 since, this only caused secondary agglomeration which made it more difficult to disperse the nanotubes. The metal decorated samples with lower CNT wt% had higher k values but those with high CNT wt% performed poorly against plain functionalized CNT samples. Shear stress experiments performed on the samples showed a weak bond between the TIM and contacting surfaces which, made it easy to remove the TIM without much force. The shearing force required to disassemble the hot pressed bond was less than one tenth of a lb as measured by the Tensile test machine. The cold pressed sample could not form a bond. Neither could the sample pressed with a

100 g weight at 100 ^{o}C.

This study was successful in creating an easy to produce polymeric based TIM with considerable higher thermal conductivity than those of earlier reported CNT-polymer composites. The materials and methods used are not expensive, complex or, time consuming. This study achieved most of the objectives of creating an ideal TIM. The best TIM made from this study had decent k values (0.72 W/m-K), a low modulus, was easy to apply and remove, cost effective, not messy to apply and, could easily deform at low pressures. Future study could be done to improve the k value by further investigating the effects of metal scattering on the phonons, better alignment techniques and, use of other metals that can be attached and, decreasing the CNT wt%.

REFERENCES

[1] F. Sarvar, D. C. Whalley, and P. P. Conway, Proceedings of the 1st Electronics System Integration Technology Conference. Dresden, Germany, 2006, (IEEE, New York, 2006) p. 1292.

[2] D. Hirschi, Semiconductor International **31,** SP2 (2008).

[3] S. Narumanchi, M. Mihalic and K. Kelly, Proceedings of the 11th IEEE Intersociety Conference on Thermal and Thermomechanical Phenomena in Electronic Systems. Orlando, 2008, (IEEE, New York, 2008) p. 395.

[4] D. Dewitt, A. S. Lavine, F. P. Incropera and T. L. Bergman, *Introduction to Heat Transfer*, 5th ed. (John Wiley & Sons, New Jersey, 2007).

[5] J. P. Gwinn and R. L. Webb, Microelectronics Journal **34,** 215 (2003).

[6] H. Fukushima, L. T. Drzal, B. P. Rook, and M. J. Rich, J. Therm. Anal. Cal. **85,** 235 (2006).

[7] S. Ijima, Nature **354,** 56 (1991).

[8] H. L. Zhang, J. F. Li, K. F. Yao and L. D. Chen, J. Appl. Phys. **97,** 114310 (2005).

[9] R. H. Baughman, A. A. Zakhidov and W.A. de Heer, Science **297,** 787 (2002).

[10] T. W. Ebbesen and P. M. Ajayan, Nature **220,** (1992).

[11] F. H. Gojny, M. H. G. Wichmann, B. Fiedler and I. A. Kinloch, Polymer **47,** 2036 (2006).

[12] D. Cai and M. Song, Carbon **46,** 2107 (2008).

[13] R. S. Prasher, X. J. Hu, Y. Chalopin, N. Mingo, K. Lofgreen, S. Volz, F. Cleri and P. Keblinski, Phys. Rev. Lett. **102,** 105901 (2009).

[14] M. Bystrzejewski, A. Huczko, H. Lange, T. Gemming, B. Buchner and M. H. Rummeli, J. Colloid Interface Science **345,** 138 (2010).

[15] V. Tzitzios, V. Georgakilas, E. Oikonomou, M. Karakassides and D. Petridis, Carbon **44,** 848 (2006).

[16] P. C. Ma, B. Z. Tang and J. K. Kim, Carbon **46,** 1497 (2008).

[17] T. Hasan, V. Scardaci, P. H. Tan, A. G.. Rozhin, W. I. Milne and A. C. Ferrari, J. Phys.Chem. C **111,** 12594 (2007).

[18] M. A. Osman and D. Srivastava, Nanotechnology **12,** 21 (2001).

[19] M. Chhowalla, K. B. K. Teo, C. Ducati, N. L. Rupesinghe, and G. A .J. Amaratunga, J. Appl. Phys. **90,** 5308 (2001).

[20] H. Huang, C. Liu, Y. Wu and S. Fan, Adv. Mater. **17,** 1652 (2005).

[21] C. I. Chen, C. Y. Ni, H. Y. Pan, C. M. Chang and D. S. Liu, Expt. Tech. **32**, 48 (2008).

[22] L. Kumari, T. Zhang, G. H. Du, W. Z. Li, Q. W. Wang, A. Datye and K. H. Wu, Composites Science and Technology **68,** 2178 (2008).

[23] Q. M. Gong, Z. Li, X. D. Bai, D. Li, Y. Zhao and J. Liang, Matl. Sci. Eng. A **384,** 209 (2004).

[24] J. Wang and J. S. Wang, Appl. Phys. Lett. **88,** 111909 (2006).

[25] C. W. Nan, G.. Liu, Y. Lin and M. Li, Appl. Phys. Lett. **85,** 3459 (2004).

APPENDIX A

Table A1 Functionalized MWCNT.

Sample #	CNT wt %	Thickness ($*10^3$mm)
34	10	.261
35	25	.127/.055
36	40	.194

Table A2 Samples with Sn@MWCNT.

Sample #	CNT:Sn Ratio	Sn@MWCNT wt%	Thickness ($*10^3$mm)
12	1:10	10	.193
13	1:10	25	.166
14	1:10	40	.196

Table A3 Samples with Cu@MWCNT.

Sample #	SDBS wt %	CNT:Cu Ratio	Cu@MWCNT wt%	Thickness ($*10^3$mm)
17	n/a	1:10	10	.143
18	n/a	1:10	25	.238
24	5	1:10	10	.186
25	25	1:10	25	.149
37	n/a	1:2	10	.231
38	n/a	1:2	25	.202
39	n/a	1:2	40	.135
43(NMP)	n/a	1:2	10	.201

Table A4 Magnetically aligned Ni@MWCNT.

Sample #	SDBS wt%	CNT:Ni Ratio	Ni@MWCNTwt%	Thickness ($*10^3$mm)
40	n/a	1:2	10	.242
41	n/a	1:2	25	.250/.197
42	n/a	1:2	40	.165/.147
54	25	1:2	5	.165

Table A5 Magnetically aligned Ni@MWCNT (2:1) with graphite and SDBS.

Sample #	SDBS wt%	Graphite wt%	Ni@MWCNT wt %	Thickness ($*10^3$mm)
58	20	1	4	.161
60	33	2	5	.22

Table A6 Magnetically aligned Cu@MWCNT (2:1) graphite and SDBS.

Sample #	SDBS wt%	Graphite wt%	Cu@MWCNT wt %	Thickness ($*10^3$mm)
59	20	1	4	.21
61	33	2	5	.133

APPENDIX B

Table B1 Thermal conductivity (k) and, standard deviation (S_x) results.

Sample #	k_1 (W/m-K)	k_2 (W/m-K)	k_3 (W/m-K)	k_{avg} (W/m-K)	S_x (σ)
12	0.255	0.358		0.307	0.073
13	0.292	0.316	0.380	0.329	0.045
14	0.331	0.351	0.350	0.344	0.011
34	0.334	0.302		0.318	0.022
35	0.257	0.324		0.291	0.047
36	0.446	0.513	0.383	0.447	0.065
17	0.198	0.227	0.302	0.242	0.053
18	0.235	0.239	0.260	0.244	0.013
24	0.246	0.275	0.320	0.280	0.037
25	0.268	0.290	0.301	0.286	0.016
37	0.264	0.234	0.286	0.261	0.026
38	0.287	0.287	0.291	0.288	0.002
39	0.261	0.298		0.279	0.026
43(NMP)	0.306	0.341		0.323	0.025
53	0.289	0.345		0.317	0.039
40	0.456	0.550		0.503	0.066
41	0.253	0.332	0.349	0.292	0.0512
42	0.179	0.336	0.371	0.257	0.102
54	0.715	0.719	0.710	0.717	0.004
49	0.408	0.382	0.438	0.423	0.027
57	0.386	0.397		0.392	0.008
58	0.621			0.621	0
59	0.537	0.542	0.553	0.544	0.007
60	0.593			0.593	0
61		0.542	0.553	0.547	0.007

VITA

Marion Odul Okoth was born in Mombasa, The Republic of Kenya. She received a B.S. degree in mechanical engineering from Minnesota State University-Mankato in 2006. She then entered the graduate program in the Mechanical Engineering Department at Texas A&M University in 2007 and received her M.S. degree in August 2010.

Contact Address: c/o Dr. Choongho Yu

Department of Mechanical Engineering,

Texas A&M University

College Station, Texas, 77843-3123

E-mail Address: odulokoth@yahoo.com